Ab Initio Calculation of Inner-Sphere Reorganization Energies of Arenediazonium Ion Couples

Michael N. Weaver,[†] Slawomir Z. Janicki,[†,‡] and Peter A. Petillo*[,†]

Roger Adams Laboratory, Department of Chemistry, University of Illinois, 600 S. Matthews Avenue, Urbana, Illinois 61801

alchmist@alchmist.scs.uiuc.edu

Received August 2, 2000

The geometries of a series of substituted arenediazonium cations (*p*-NO_2, *p*-CN, *p*-Cl, *p*-F, *p*-H, *m*-CH_3, *p*-CH_3, *p*-OH, *p*-OCH_3, *p*-NH_2) and the corresponding diazenyl radicals were optimized at the HF/6-31G*, MP2/6-31G*, B3LYP/6-31G*, B3LYP/TZP, B3PW91/TZP, and CASSCF/6-31G* levels of theory. Inner-sphere reorganization energies for the single electron-transfer reaction between the species were computed from the optimized geometries according to the NCG method and compared to experimental values determined by Doyle et al. All levels of theory predicted a CNN bond angle of 180° in the cation. A bent neutral diazenyl radical was predicted at all levels of theory excepting B3LYP/TZP and B3PW91/TZP for the *p*-Cl-substituted compound. Inner-sphere reorganization energies determined at the HF, MP2, and CASSCF levels of theory correlated poorly with both experimental results and calculated geometries. Density functional methods correlated best with the experimental values, with B3LYP/6-31G* yielding the most promising results, although the ROHF/6-31G* survey also showed some promise. B3LYP/6-31G* calculations correctly predicted the order of the inner-sphere reorganization energies for the series, excluding the halogen-substituted compounds, with values ranging from 42.8 kcal mol^{-1} for the *p*-NO_2-substituted species to 55.1 kcal mol^{-1} for NH_2. The magnitudes of these energies were lower than the experimental by a factor of 2. For the specific cases examined, the closed-shell cation geometries showed the expected geometry about the CNN bond, with variations in the CN and NN bond lengths correlating with the electron-donating/withdrawing capacity of the substituent. As predicted by Doyle et al., a large geometry change was observed upon reduction. The neutral diazenyl radicals showed a nominal CNN bond angle of 120° and variations in the CN and NN bond lengths also correlated with the electron-donating/withdrawing capacity of the substituent. Changes in θ_{CNN} and r_{CN} both correlated well with calculated λ_{inner}. The key parameters influencing inner-sphere reorganization energy were the CN and NN bond lengths and the CNN bond angle. This influence is explained qualitatively via resonance models produced from NRT analysis and is related to the amount of CN double bond character. Based on these observations, B3LYP/6-31G* calculations are clearly the most amenable for calculating inner-sphere reorganization energies for the single electron-transfer reaction between cation/neutral arenediazonium ion couples.

Introduction

Reduction of arenediazonium salts provides the basis for a substantial number of chemical reactions.[1] One notable application is the Sandmeyer reaction,[2] which utilizes the diazo moiety to facilitate functionalization of aromatic systems and remains one of the most reliable transformations in organic chemistry.[3,4] The general reaction involves the addition of the cuprate salt of the desired moiety to the diazonium species (eq 1).

$$ArN_2^+ + CuX \rightarrow ArX \qquad (1)$$

A large body of literature investigating the mechanism of the Sandmeyer reaction exists, and as early as 1942, one-electron processes were thought to dominate the mechanistic pathway.[5] Kochi furthered this mechanistic interpretation,[2b] and the current consensus remains that the reaction proceeds via single electron transfer (SET).[4] Eberson has summarized several models for studying electron-transfer reactions including the thermodynamic approach, the Single Electron Shift, Marcus Theory for Outer-sphere electron transfer, Hush theory, and two kinetic models.[6] Of these, Marcus theory is perhaps the most well-known, most often used to describe organic reactions and is a particularly amenable model for

* To whom correspondence should be addressed. Tel no: (217) 333-0695. FAX no: (217) 244-8559.
† University of Illinois.
‡ Current Address: Narchem Corp., 3800 W. 38th St., Chicago, IL 60632.

(1) Kochi, J. K. *Organometallic Mechanisms and Catalysis*; Academic Press: New York, 1978; Chapter 9.

(2) (a) Doyle, M. P.; Siegfried, B.; Dellaria, J. F., Jr. *J. Org. Chem.* **1977**, *42*, 2426. (b) Kochi, J. K. *J. Am. Chem. Soc.* **1957**, *79*, 2942. (c) Jenkins, C. L.; Kochi, J. K. *Ibid.* **1972**, *94*, 956. (d) Harrington, P. J.; Hegedus, L. S. *J. Org. Chem.* **1984**, *49*, 2657. (e) Wulfman, D. S. In *The Chemistry of Diazonium and Diazo Groups*; Patai, S., Ed.; Wiley: New York, 1978; Part 1, Chapter 8.

(3) Kornblum, N. In *Organic Reactions, Volume II*; Adams, R.; Bachman, W. E.; Fieser, L. F.; Johnson, J. R.; Snyder, H. R., Eds.; Wiley: New York, 1944; Chapter 7.

(4) Galli, C. *Chem. Rev.* **1988**, *88*, 765 and references contained therein.

(5) Waters, W. A. *J. Am. Chem. Soc.* **1942**, *64*, 266.

(6) Eberson, L. *Electron-Transfer Reactions in Organic Chemistry*; Springer-Verlag: Heidelberg, 1987 and references therein.

10.1021/jo0011742 CCC: $20.00
Published on Web 01/30/2001

investigating SET processes by molecular orbital calculations.[7−10]

According to Marcus theory,[11,12] the reorganization energy of a system upon SET, λ, is broken down into two terms: the "inner," λ_{inner}, and "outer," λ_{outer} components. The λ_{inner} term accounts for the bond lengths, angles, and torsions, which must be modified in order to satisfy the geometric requirements for the electron transfer. The λ_{outer} term accounts for solvation that further alters the electrostatic environment about transfer partners. In gas-phase electron-transfer reactions, the solvent term can be ignored, leaving changes in internal geometry the sole determinant of λ.[6,8,10]

The transfer of a single electron is either an outer sphere or inner sphere process.[6] The outer sphere process involves transfer of the electron between two separate primary bond systems (eq 2), while the inner sphere process is characterized by the formation of a bonded intermediate which subsequently effects the electron transfer through homolytic bond cleavage (eq 3).

$$R_1^+ + R_2^\bullet \rightarrow R_1^\bullet + R_2^+ \quad (2)$$

$$R_1^+ + R_2^\bullet \rightarrow [R_1{-}R_2]^{+\bullet} \rightarrow R_1^\bullet + R_2^+ \quad (3)$$

The structure and reactivity of arenediazonium ions have a direct bearing on the mechanism of the Sandmeyer reaction. During this reaction, a single electron is initially transferred to the diazonium cation to produce a neutral, diazenyl radical. This species readily loses nitrogen to produce an aryl radical that subsequently combines with the "X" portion of the cuprate salt.[2b]

Doyle et al. determined that the reduction of arenediazonium tetrafluoroborate salts is an outer-sphere electron-transfer process.[13] They utilized potassium ferrocyanide and decamethylferrocene as reducing agents to transfer a single electron to a series of *meta*- and *para*-substituted arenediazonium ions (Figure 1). Marcus theory was applied to obtain an estimate of the apparent self-exchange rate constant for the cross-reaction between the arenediazonium cation and its reduced, neutral counterpart. The apparent self-exchange rate constants for electron transfer between the two species were then utilized to determine the reorganization energies for the SET reaction between the cation/neutral species. The rate data also allowed for the evaluation of $\Delta G^\dagger$ and λ for each process (eq 4). In the case of a self-exchange process, eq 4 further simplifies as $\Delta G° = 0$.

$$\Delta G^\dagger = \frac{\lambda}{4}\left(1 + \frac{\Delta G°}{\lambda}\right) \quad (4)$$

The apparent self-exchange rate constants for single electron transfer between cation/neutral couples of these arenediazonium ions showed a substantial substituent influence ($\rho = +6.4$).[13] The rate of outer-sphere one electron reduction is also influenced by the electron-withdrawing capacity of the substituent, with experimental Hammett ρ values established to range from +3.3 to +4.7 depending upon the reducing agent employed.[13] Doyle et al. also reported experimental reorganization energies ranging from 80 kcal mol^{-1} for a *p*-Cl-substituted arenediazonium species to 89 kcal mol^{-1} for the *p*-OCH_3 derivative. The magnitude of λ across the series forced the conclusion that the geometries of the cation and neutral[14] species must be substantially different.

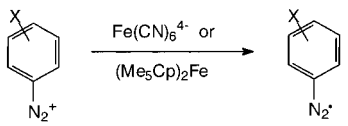

Entry	X	$FeCN_6^{4-}$ 10^{-2} k_x, M^{-1} s^{-1}	$(Me_5Cp)_2Fe$ 10^{-3} k_x, M^{-1} s^{-1}
1	*p*-NO_2	695	*a*
2	*p*-CN	103	*a*
3	*p*-Cl	2.76	305
4	*p*-F	0.526	76.4
5	*p*-H	0.227	61.1
6	*m*-CH_3	0.0843	34.0
7	*p*-CH_3	0.0206	11.0
8	*p*-OH	n/d[b]	n/d[b]
9	*p*-OCH_3	0.0071	8.58
10	*p*-NH_2	n/d[b]	n/d[b]

[a] Too fast to measure. [b] Not determined experimentally, but included as part of this investigation.

Figure 1. Cross-coupling rate constants determined by Doyle et al. with (a) potassium ferrocyanide and (b) decamethylferrocene.

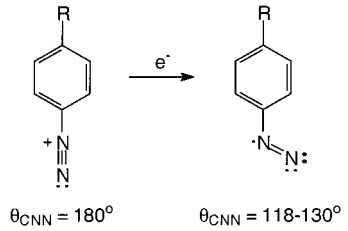

Figure 2.

Marcus theory predicts that changes in the structure of the diazonium cation/neutral couple directly relate to the rate of electron transfer, since reduction requires a geometry change about the diazo moiety (Figure 2). The geometry modification likely involves substantial variations in the CN and NN bond lengths of the diazo moiety as well as the obvious change in the CNN bond angle. Other changes in the arene structure also occur and will affect the overall rate. Marcus theory therefore suggests that evaluation of the composite geometry changes between coupling partners *in the gas phase* is equivalent to λ_{inner} (to a first approximation). In turn, this value is directly related to $\Delta G^\dagger$ for the self-exchange process (eq 4).

λ_{inner} can be calculated using a harmonic oscillator model for inner-shell vibrations.[15] Force constants for bond stretching (IR spectroscopy) and changes in the equilibrium bond lengths (X-ray crystallographic analysis) for each molecular vibration are needed for the two oxidation states in the ET couple. These force constants

(7) Nelsen, S. F.; Blackstock, S. C.; Kim, Y. *J. Am. Chem. Soc.* **1987**, *109*, 677.
(8) Petillo, P. A.; Nelsen, S. F. *Abstr. Pap. Am. Chem. Soc.* **1992**, *204*, 381.
(9) Eberson, L.; Gonzalez-Luque, R.; Lorentzon, J.; Merchan, M.; Roos, B. O. *J. Am. Chem. Soc.* **1993**, *115*, 2898.
(10) Petillo, P. A., Ph.D. Thesis, University of Wisconsin—Madison, 1991.
(11) Marcus, R. A. *Discuss. Faraday Soc.* **1960**, *57*, 557.
(12) (a) Marcus, R. A. *J. Chem. Phys.* **1956**, *24* (5), 966. (b) Marcus, R. A. *J. Chem. Phys.* **1956**, *24* (5), 979.
(13) Doyle, M. P.; Guy, J. K.; Brown, K. C.; Makapatro, S. N.; VanZyl, C. M.; Pladziewicz, J. R. *J. Am. Chem. Soc.* **1987**, *109*, 1536.
(14) The neutral species is the diazenyl radical corresponding to the respective cation.
(15) Sutin, N. *Acct. Chem. Res.* **1968**, *1*, 225. (b) Sutin, N. *Acct. Chem. Res.* **1982**, *15*, 275.

are usually estimates for all but the simplest systems where the number of molecular vibrations is finite and discernible.

The most direct computational approach for evaluating λ_{inner} is the NCG method described by Nelsen, Blackstock, and Kim.[7,16] The method is based upon the energetic relationship of the species in an idealized self-ET reaction, where λ is the vertical transition when an electron is moved between ground-state geometries without geometry relaxation. This is evaluated by determining the equilibrium geometry and energy for each reacting partner followed by single point calculations in the equilibrium geometries with altered charge and multiplicity.[17] The sum of the two vertical ionization energies is λ_{inner}. Thus, the enthalpy portion of λ is simply the sum of the relaxation energies for the two vertical transitions of each reactant in the ET couple, and determination of these energies is well suited for computation. In principle, virtually any molecular orbital treatment can be used, but a model should be chosen that correctly reproduces the salient features of the geometry of both oxidation states. One distinct advantage of this approach is that compounds that are difficult or impossible to study experimentally may be investigated using this approach.

To date, theoretical investigations on arenediazonium species remain limited.[18−22] Glaser and co-workers investigated the bonding in diazonium species,[18] diazonium ion behavior in amino acids and in dediazonation reactions,[19,20] and the stability of alkyldiazonium ions[21] in biological systems. They also investigated the structures of arenediazonium cations,[19,22] but no calculations on the neutral diazonium species have been conducted and theoretical reorganization energies have yet to be determined.

Herein, we report λ_{inner} values for a series of substituted arenediazonium self-exchange couples and quantify the changes in geometry that occur upon SET. The dependence of λ_{inner} on the substituent electron-withdrawing/donating capacity is compared to the experimental values of Doyle et al.[13] Finally, a survey of several modern ab initio methods is presented and the efficacy of each approach evaluated in light of the experimental data of Doyle et al.

Computational Methods

All HF and DFT calculations utilized the Gaussian 92 and 94 suite of programs on an RS6000/SP2 computer.[23,24] Full π-complete active space SCF (CASSCF) calculations were performed using the PC GAMESS version of the GAMESS (US) QC package.[25] Closed-shell systems utilized the spin-restricted Hartree−Fock (RHF) approximation. Open-shell system calculations with the 6-31G* basis set[26] utilized both the unrestricted Hartree−Fock (UHF) and spin-restricted open-shell Hartree−Fock (ROHF) approximations.

Triple-ζ basis set calculations utilized the contractions of Dunning and Huzinaga and are properly a double-ζ core and a full triple-ζ valence shell with different *s* and *p* coefficients.[27] One set of Cartesian *d*-type polarization functions for both nitrogen and hydrogen augmented the triple-ζ basis set, termed the TZP basis set. An orbital exponent of 0.80 was used for nitrogen; 1.1 was used for hydrogen. All Moller−Plesset second-order perturbation corrections (MP2) included core orbitals. The density functionals B3LYP and B3PW91 were used as implemented in Gaussian 94.[28,29,30]

Geometry optimizations utilized standard gradient methods for all single-configuration SCF, DFT, MP2, and π-CASSCF optimizations. Frequency analysis of the optimized HF/6-31G* cation and neutral geometries revealed no negative frequencies. Memory considerations precluded the completion of these calculations at the MP2/6-31G* level of theory. Natural Bond Orbital (NBO) and Natural Resonance Theory (NRT) analyses utilized NBO 4.0[31] as implemented in Gaussian 94.[32] Orbitals produced from Gaussian 92/94 and PC-GAMESS runs were viewed using the MOLDEN[33] package for viewing molecular density.[34]

(16) The term NCG is an abbreviation for Neutral in Cation Geometry. The two vertical ionization energies are the neutral in the cation geometry and the cation in the neutral geometry, hence the abbreviation.

(17) Upon changing from the cation or neutral optimized geometries, it is not necessary to make any assumptions about the shape of the potential energy surfaces. Eberson has shown that this is an artifact of the chosen methodology for evaluating λ_{inner}. See ref 9 for further details.

(18) Glaser, R.; Horan, C. J.; Lewis, M.; Zollinger, H. *J. Org. Chem.* **1999**, *64*, 902.

(19) Glaser, R.; Son, M.-S. *J. Am. Chem. Soc.* **1996**, *118*, 10942.

(20) Glaser, R.; Rayat, S.; Lewis, M.; Son, M.-S.; Meyer, S. *J. Am. Chem. Soc.* **1999**, *121*, 6108.

(21) Glaser, R.; Choy, G. S.-C.; Hall, M. K. *J. Am. Chem. Soc.* **1991**, *113*, 1109.

(22) Glaser, R.; Horan, C. J. *J. Org. Chem.* **1995**, *60*, 7518.

(23) Frisch, M. J.; Trucks, G. W.; Schlegel, H. B.; Gill, P. M. W.; Johnson, B. G.; Wong, M. W.; Foresman, J. B.; Robb, M. A.; Head-Gordon, M.; Replogle, E. S.; Gomperts, R.; Andres, J. L.; Raghavachari, K.; Binkley, J. S.; Gonzalez, C.; Martin, R. L.; Fox, D. J.; Defrees, D. J.; Baker, J.; Stewart, J. J. P.; Pople, J. A. Gaussian 92/DFT, Revision G.3, Gaussian, Inc., Pittsburgh, PA, 1993.

(24) Frisch, M. J.; Trucks, G. W.; Schlegel, H. B.; Gill, P. M. W.; Johnson, B. G.; Robb, M. A.; Cheeseman, J. R.; Keith, T.; Petersson, G. A.; Montgomery, J. A.; Raghavachari, K.; Al-Laham, M. A.; Zakrzewski, V. G.; Ortiz, J. V.; Foresman, J. B.; Cioslowski, J.; Stefanov, B. B.; Nanayakkara, A.; Challacombe, M.; Peng, C. Y.; Ayala, P. Y.; Chen, W.; Wong, M. W.; Andres, J. L.; Replogle, E. S.; Gomperts, R.; Martin, R. L.; Fox, D. J.; Binkley, J. S.; Defrees, D. J.; Baker, J.; Stewart, J. P.; Head-Gordon, M.; Gonzalez, C.; Pople, J. A. Gaussian 94, Revision D.3, Gaussian, Inc., Pittsburgh, PA, 1995.

(25) PC-GAMESS is an optimized version of GAMESS for Windows-NT written and maintained by Alex A. Granovsky, The executable can be obtained free of charge at www http://classic.chem.msu.su/gran/gamess/index.html. For a complete description of GAMESS, see: Schmidt, M. W.; Boatz, J. A.; Baldridge, K. K.; Kosekim S.; Gordon, M. S.; Elbert, S. T. *QCPE Bull.* **1987**, *7*, 115.

(26) For references describing the standard abbreviations and basic ab initio methods, see the following: (a) Hehre, W. J.; Radom, L.; Schleyer, P. v. R.; Pople, J. A. *Ab initio Molecular Orbital Theory*; Wiley-Interscience: New York, 1986. (b) Clark, T. *A Handbook of Computational Chemistry*; Wiley-Interscience: New York, 1985.

(27) (a) Huzinaga, S. *J. Chem. Phys.* **1965**, *42*, 1293. (b) Dunning, T. H., Jr. *J. Chem. Phys.* **1971**, *55*, 716. (c) Dunning, T. H.; Hay, P. J. *Modern Theoretical Chemistry*, Plenum: New York, 1976; pp 1−28.

(28) Becke, A. D. *J. Chem. Phys.* **1993**, *98*, 5648.

(29) For references detailing the three-component functionals, see: (a) Becke, A. D. *Phys. Rev. A* **1988**, *38*, 3098. (b) Lee, C.; Yang, W.; Parr, R. G. *Phys. Rev. B* **1988**, *37*, 785. (c) Vosko, S. H.; Wilk, L.; Nusair, M. *Can. J. Phys.* **1980**, *58*, 1200.

(30) For references on the gradient-corrected correlation functional, see: (a) Wang, Y.; Perdew, J. P. *Phys. Rev. B* **1991**, *44*, 13298. (b) Perdew, J. P.; Wang, Y. *Phys. Rev. B* **1992**, *45*, 13244.

(31) NBO 4.0. E. D. Glendening, J. K. Badenhoop, A. E. Reed, J. E. Carpenter, and F. Weinhold, Theoretical Chemistry Institute, University of Wisconsin, Madison, WI, 1996.

(32) For those compounds containing large numbers of resonance structures, the available memory was increased to 20 megawords and the threshold was raised to ∼10% of the strongest interaction observed in perturbation theory analysis using the NRTTHR keyword. In the case of compound **3**, this interaction was found to be 155 kcal mol^{-1} in the cation; for compound **6** (cation) the largest interaction was 305 kcal mol^{-1}. In addition to altering the threshold, the reference structures for $\mathbf{6}^{+}$ were necessarily defined with the $NRTSTR keyword. All other entries were analyzed successfully using the default parameters.

(33) Schaftenaar, G.; Noordik, J. H. Molden: a pre- and post-processing program for molecular and electronic structures. *J. Comput.-Aided Mol. Des.* **2000**, *14*, 123.

(34) In instances where imaginary frequencies were produced (indicating the geometry resides at a local as opposed to a global minimum), MOLDEN was utilized in order to elucidate any necessary structural adjustments for obtaining the optimized geometry. Orbitals included and discussed herein are shape orbitals with a contour value of 0.05 applied in MOLDEN.

Table 1. 6-31G* Calculated λ_{Inner} Values for 1−10 (all values in kcal mol^{-1})

entry	substituent	UHF[a]	ROHF	MP2	B3LYP
1	NO_2	84.2	71.9	37.5	42.8
2	CN	83.5	71.3	45.5	42.9
3	Cl	82.7	73.4	41.8	64.9
4	F	83.6	75.3	44.5	49.7
5	H	83.4	73.2	59.5	47.3
6	m-CH_3	85.1	73.2	41.8	47.4
7	p-CH_3	83.6	73.4	61.0	47.6
8	OH	83.2	76.5	47.5	51.3
9	OCH_3	83.8	77.2	48.1	51.8
10	NH_2	82.8	78.0	50.8	55.1

[a] UHF/ROHF designations refer to the optimized neutral geometry used for the vertical calculation.

Table 2. DFT/TZP and π-CASSCF/6-31G* Calculated λ_{Inner} Values for 1−10 (all values in kcal mol^{-1})

entry	substituent	B3LYP	B3PW91	π-CASSCF/6-31G*
1	NO_2	43.2	42.2	- - -
2	CN	42.3	41.8	72.6
3	Cl	8.1	7.9	72.2
4	F	139.2	46.2	72.4
5	H	46.7	46.3	72.4[a]
6	m-CH_3	46.7	46.3	72.2
7	p-CH_3	47.2	46.8	71.7
8	OH	50.8	50.5	71.8
9	OCH_3	51.2	50.9	68.6
10	NH_2	53.5	53.2	60.2

[a] Value reported is for calculations performed with and without *n* pairs.

Table 3. Comparison of Theoretical and Available Experimental Results (all values in kcal mol^{-1}) for Compounds Studied by Doyle et al.[13]

			6-31G*				
entry	substituent	expntl[a]	UHF	ROHF	MP2	DFT	CASSCF
3	Cl	80.1	82.7	73.4	41.8	64.9	72.2
4	F	85.3	83.6	75.3	44.5	49.7	72.4
5	H	83.8	83.4	73.2	59.5	47.3	72.4
6	m-CH_3	86.0	85.1	73.0	41.8	47.4	72.2
7	p-CH_3	88.7	83.6	73.3	61.0	47.6	71.7
9	OCH_3	89.0	83.8	77.2	48.1	51.8	68.6

Results and Discussion

The geometries of the cation and neutral species for compounds **1**−**10** (Figure 1) were optimized with a range of popular computational methods, the vertical transitions evaluated, and λ_{inner} values determined by the NCG method.[7] λ_{inner} values are shown at the HF/6-31G*, MP2/6-31G*, B3LYP/6-31G*, B3LYP/TZP, B3PW91/TZP, and CASSCF/6-31G* levels of theory (Tables 1−3).

The experimental values established by Doyle et al.[13] provide the basis for evaluating the theoretical λ_{inner} values and trends. In general, the computational models employed in this study fail to reproduce the experimentally derived λ_{inner} trends either in magnitude or order based on substituent (Table 3, Figure 1). Only the UHF/6-31G* λ_{inner} values are computed to be in the same range as those reported by Doyle et al., but the rank order correlates poorly with substituent and experimental rate constant (Tables 1−3, Figure 1). The DFT/6-31G* λ_{inner} values and the MP2/6-31G* energies are lower than the experimental values by nearly a factor of 2.[35] The ROHF-derived λ_{inner} values are lower than the respective UHF values by 10%.

The inability of these models to accurately reproduce the magnitude of λ_{inner} is likely due to the nature of the experimental data and the tacit assumption that $\lambda \cong \lambda_{inner}$.[36] Clearly, a solvent organization term (λ_s) exists, although its exact magnitude is difficult to assess.[6] The experimental reorganization energies, λ, (which include both λ_{inner} and λ_s terms) of Doyle et al. were extracted from cross-reaction rate constants and thus are dependent upon published $E°$ values. Doyle et al. utilized $E°$ values determined in sulfolane[37] (the only consistent data set for the entire series of diazonium cations) that are 0.03 to 0.2 eV higher than the corresponding $E°$ values in water and acetonitrile (the solvents used in the experimental study).[13] Lowering of a redox potential by 0.1 eV can result in a 10 kcal mol^{-1} decrease in the corresponding λ. For experiments conducted in water, λ_s can easily be 10−20 kcal mol^{-1} and thus may account for a substantial part of the total reorganization energy.[6] Due to the fact that the λ_s terms and $E°$ values recorded in the experimental solvent are not available for these systems, it is not possible to ascertain the exact uncertainty in the experimental data.[38]

Both HF models and the MP2/6-31G* results fail to properly order the resulting λ_{inner} values in order of increasing donating ability. For example, **9** has a smaller λ_{inner} value compared to **1**, which is quite opposite the experimental observation. MP2/6-31G* λ_{inner} values are widely scattered with respect to substituent donor/acceptor ability. Similar problems are associated with the λ_{inner} trends computed at π-CASSCF/6-31G*, where the trends exactly oppose the experimental results. No CASSCF data for **1** is available, as the π-system proved too large to calculate in PC-GAMESS. The ROHF numbers exhibit the expected general trend, but the data are not uniform.

The ROHF/6-31G* data and those derived from density functional methods correlate the best, with B3LYP/6-31G* providing the best overall evaluation of the experimental trends (Figure 3). None of the methods employed appear to handle **3** and **4** particularly well, with the density functional methods clearly ill-suited for these species. Problems in treating halides, especially F^-, with DFT methods have been noted,[39] and consequently our observations may not be too surprising. We also encountered similar problems with the *p*-Br substituent (data not shown), in that the calculated λ_{inner} values were substantially larger than the *p*-NH_2 species. Although the data for **4** is not grossly out of line for B3LYP/6-31G*, the other DFT calculations are clearly in error. Given that the halides **3** and **4** in this study may present special problems, all subsequent analyses will exclude data for these compounds. Many of the models also appear to incorrectly suggest that the *p*-CN derivative **2** should have a faster rate constant and lower λ_{inner} than **1**, which is opposite of the experimental observations. No clear

(35) The experimental numbers determined by Doyle et al. were extrapolated from the apparent self-exchange rate constants based on the decamethylferrocene−arenediazonium rate data. Reorganization energies ranged from 80 kcal/mol for the *p*-Cl derivative to 89 kcal/mol for the *p*-OCH_3 compound. For details on the calculations required for determining the experimental reorganization energy, see ref 13.

(36) We acknowledge both reviewers for bringing these details to our attention.

(37) Elofson, R. M. *J. Org. Chem.* **1969**, *34*, 3335.

(38) One reviewer correctly suggested that remeasurement of the $E°$ values utilizing modern electrochemical techniques may reduce experimental uncertainty and narrow the gap between calculated and experimental reorganization energies.

(39) (a) Jarecki, A. A.; Davidson, E. R. *Chem. Phys. Lett.* **1999**, *300*, 44. (b) Curtiss, L. A.; Redfern, P. C.; Raghavachari, K.; Pople, J. A. *J. Chem. Phys.* **1998**, *109*, 42. (c) Tschumper, G. S.; Schaefer, H. F., III. *J. Chem. Phys.* **1998**, *107*, 2529.

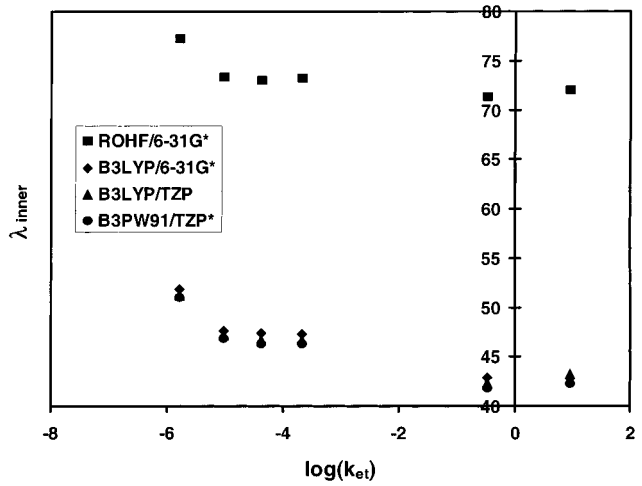

Figure 3. Correlation of calculated λ_{inner} with experimental rate data. Note that data for **3** and **4** are excluded.

reason for this disparity is available from the wave functions or geometries (vide infra).

Eberson[9] has noted the sensitivity of λ_{inner} as a function of computational model, an observation we made independently and prior to Eberson's discussion.[8,10] Accurate determination of λ_{inner} values requires that the computational model fulfill two criteria: (1) an accurate description of the wave function for both species, and (2) an accurate depiction of the two ground-state geometries. The best computational methodologies combine these two features and provide the best modeling of λ_{inner}. For small molecules such as NO and NO_2, we and Eberson independently concluded that full valence CASSCF calculations with a reasonable basis set are needed to accurately describe λ_{inner}. For other systems where full valence CASSCF calculations are computationally intractable (such as **1**−**10**), simpler models must be employed. Clearly, the models utilized in this study fail in at least one of these criteria.

Open-shell species are known to pose special problems when modeled due to the multiconfigurational nature of such systems. Methods such as HF and MP2 are known to have difficulty correctly describing the salient features of open-shell systems, as spin contamination from higher states often mixes into the ground-state wave function.[40] DFT methods have been shown to have some advantages for many open-shell species.[41] For **1**−**10**, the degree of spin contamination, described as a deviation of $S(S + 1)$ from the idealized 0.75 for a doublet state, is substantial, with values up to 1.3 observed in some cases. By contrast, the values of $S(S + 1)$ for B3LYP/6-31G* are between 0.75 and 0.756. Additionally, the ROHF/6-31G* model forces the wave function into a pure doublet state, which may reflect why these models provide a better correlation with the experimental trends. The failure to accurately model λ_{inner} is most likely related to a poor electronic description of the open-shell neutral diazenyl radical

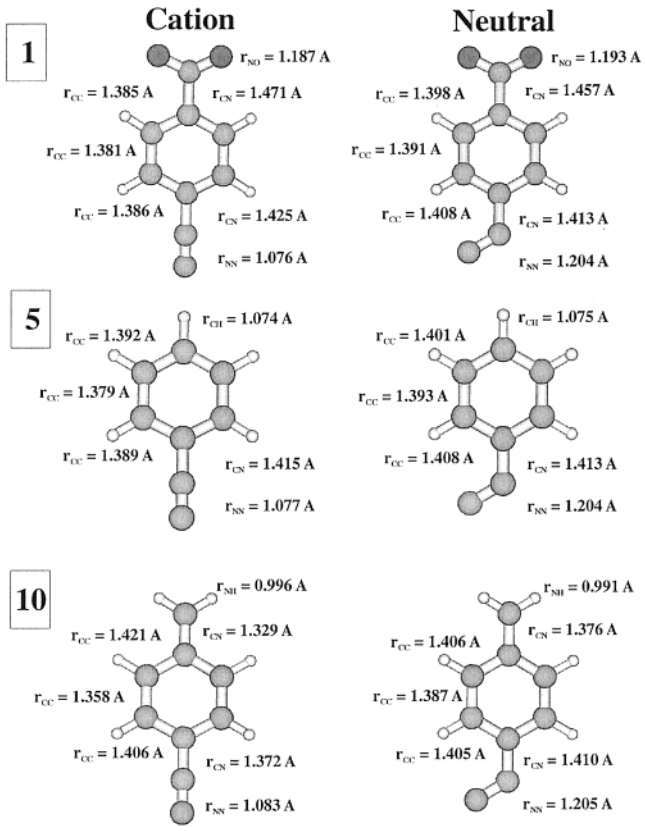

Figure 4. Summary of B3LYP/6-31G* optimized bond lengths for **1**, **5**, and **10** cations and neutrals.

ground state, as the description of the closed-shell diazonium cation should not be problematic. We conclude that the best method for evaluating λ_{inner} *trends* for this and related systems is B3LYP/6-31G*, although the results should be used with caution. A scaling factor would be necessary were this model to be used to evaluate absolute λ_{inner} values.

Despite the obvious shortcoming of the methods employed in this study, the ROHF/6-31G* and all the DFT data sets predict that the *p*-aminobenzenediazonium species will have the largest λ_{inner} value, and consequently the slowest rate. These models also predict that the *p*-hydroxybenzenediazonium (not studied experimentally) will have a slightly smaller λ_{inner} and therefore a slightly faster rate compared to the anisole derivative. As expected from the large λ_{inner} values, a substituent's donor/acceptor abilities also affect many of the key geometric parameters (e.g., r_{CN}, r_{NN}, θ_{CNN}).

As expected, the RHF/6-31G* geometries of cations **1**, **5**, and **10** compare favorably with those published by Glaser et al.,[42] with the deviation in bond lengths at most 0.004 Å and in bond angle at most 0.1° with the majority of the data virtually comparable. The optimized cation and neutral geometries do reveal dramatic absolute changes in the optimized geometry as a function of computational model, although data within a particular model are consistent as a function of substituent donor/acceptor abilities (see Supporting Information for a complete summary of molecular geometries). The key bond lengths (Figure 4) and bond angles (Figure 5) from

(40) Jungwirth, P.; Bally, T. *J. Am. Chem. Soc.* **1993**, *115*, 5783.

(41) (a) Li, J. B.; Cramer, C. J.; Truhlar, D. G. *Biophys. Chem.* **1999**, *78*, 147. (b) Cramer, C. J.; Nash, J. J.; Squires, R. R. *Chem. Phys. Lett.* **1997**, *277*, 311. (c) Worthington, S. E.; Cramer, C. J. *J. Phys. Org. Chem.* **1997**, *10*, 755. (d) Lim, M. H.; Worthington, S. E.; Dulles, F. J.; Cramer, C. J. Density-functional calculations of radicals and diradicals. In *Chemical Applications of Density Functional Theory*; ACS Symposium Series, American Chemical Society: Washington, DC, 1996; pp 402−422.

(42) Glaser, R.; Horan, C.; Zollinger; H. *Angew. Chem., Int. Ed. Engl.* **1997**, *36*, 2210.

Table 4. θ_{CNN} (reported in degrees) for Diazenyl Neutral Radicals 1−10

		6-31G*				TZP		
entry	substituent	UHF[a]	ROHF	MP2	B3LYP	B3LYP	B3PW91	CASSCF
1	NO_2	120.9	122.3	126.6	124.3	124.6	124.5	- - -
2	CN	121.0	122.4	126.8	124.5	125.0	125.0	123.7
3	Cl	121.1	122.7	127.5	124.9	180.0	180.0	123.5
4	F	121.2	122.9	127.9	125.0	125.0	125.0	124.0
5	H	121.3	122.9	130.0	125.0	125.5	125.4	124.1
6	m-CH_3	120.7	122.9	127.5	125.0	125.5	125.4	124.1
7	p-CH_3	120.7	122.9	129.9	125.1	125.6	125.6	124.1
8	OH	121.3	123.1	128.7	125.3	125.8	125.7	124.1
9	OCH_3	121.4	123.1	128.8	125.3	125.8	125.8	124.1
10	NH_2	121.5	123.4	130.2	125.5	126.1	126.1	124.4

[a] UHF/ROHF designations refer to the optimized neutral geometry.

Table 5. Summary of Important B3LYP/6-31G* Cation and Neutral Bond Lengths and Bond Length Differences for 1−10

		r_{CN}			r_{NN}			r_{CX}		
entry	substituent	C	N	Δ_{CN}	C	N	Δ_{NN}	C	N	Δ_{CX}
1	NO_2	1.381	1.457	0.076	1.114	1.186	0.072	1.494	1.476	−0.018
2	CN	1.375	1.455	0.080	1.116	1.186	0.070	1.429	1.434	0.005
3	Cl	1.368	1.452	0.084	1.117	1.187	0.070	1.715	1.753	0.038
4	F	1.368	1.451	0.083	1.117	1.187	0.070	1.316	1.346	0.030
5	H	1.374	1.454	0.080	1.115	1.187	0.072	1.086	1.086	0.000
6	m-CH_3	1.373	1.454	0.081	1.116	1.187	0.071	1.505	1.511	0.006
7	p-CH_3	1.367	1.451	0.084	1.120	1.187	0.067	1.500	1.510	0.010
8	OH	1.359	1.446	0.087	1.120	1.188	0.068	1.326	1.362	0.036
9	OCH_3	1.357	1.446	0.089	1.121	1.188	0.067	1.319	1.359	0.040
10	NH_2	1.349	1.443	0.094	1.124	1.189	0.065	1.339	1.388	0.049

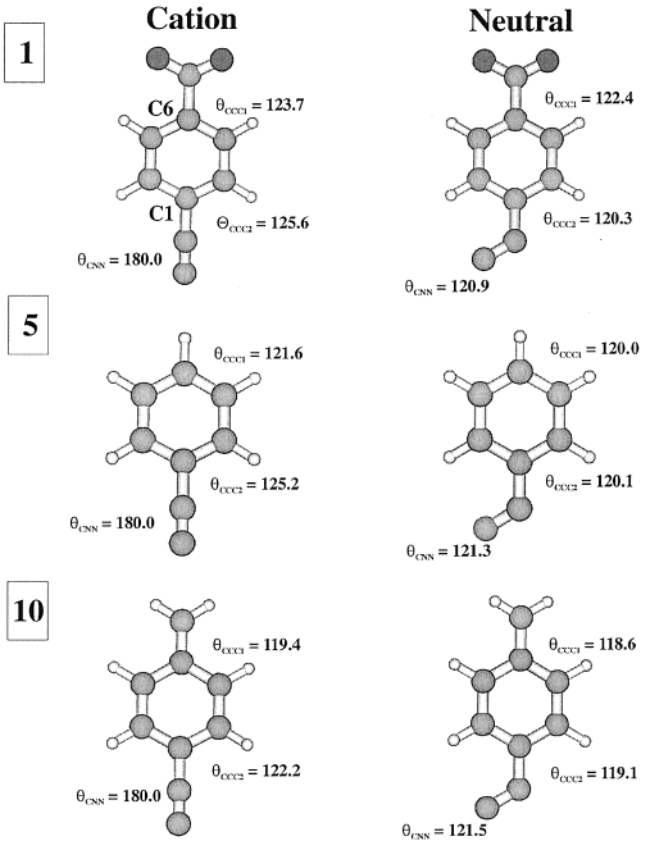

Figure 5. Summary of B3LYP/6-31G* optimized bond angles for **1**, **5** and **10** cations and neutrals.

the B3LYP/6-31G* optimizations are summarized for **1**, **5**, and **10**.

A substantial change in geometry is observed upon reduction of the cation to the neutral diazenyl radical. This is consistent with the conclusion of Doyle et al. that the structures of the cation and neutral species are substantially different. θ_{CNN} in the cation has the expected value of 180° at all levels of theory. Due to the presence of an unpaired electron on the central nitrogen, the bond angles in the neutral species deviate from 180° (Table 4). In all cases (with the exception of two DFT calculations on **3**), θ_{CNN} for the neutral diazenyl radical is bent, with a nominal value of 120°.

The DFT/TZP optimizations of **3** are clearly wrong, as θ_{CNN} is not 180°, but no obvious explanation for this anomalous behavior is readily apparent. While this vast geometric disparity suggests a possible explanation for the poor modeling of λ_{inner}, all other computed geometries of **3** and **4**, including θ_{CNN}, are reasonably consistent with the trend observed for the other compounds. Examination of the differences in bond lengths Δ_{CX} (Table 5) between the cation and neutral for **3** and **4** suggests that the failure to accurately model λ_{inner} is due to a poor description of the r_{CX} between oxidation states. At the B3LYP/6-31G* level, Δ_{CX} is found to be too large in comparison to the other species, reinforcing our earlier hypothesis that the DFT methods may be ill-suited for these halogen-substituted compounds.

Comparison of **5** with the other compounds in the series reveals the expected influence of electron-donating and -withdrawing substituents on r_{CN}, r_{NN}, and θ_{CNN} (Tables 5 and 6). Changes in r_{CN}, r_{NN}, and θ_{CNN} upon reduction (Tables 5 and 6) correlate well with λ_{inner}. Excluding data for **3** and **4**, the cation r_{CN} ($R^2 = 0.92$), neutral r_{CN} ($R^2 = 0.91$), and neutral θ_{CNN} ($R^2 = 0.92$) show the expected trends with λ_{inner} (Figures 6 and 7). Calculations at the B3LYP/TZP and B3PW91/TZP levels fare slightly worse, with R^2 values of 0.87 and 0.83 for r_{CN} and 0.89 and 0.88 for θ_{CNN}, respectively.

θ_{CNN} for the neutrals with electron-donating substituents is larger than for the corresponding withdrawing group-substituted species. One of the more substantial structural effects occurs in the CCC bond angles centered

Table 6. Summary of Important B3LYP/6-31G* Cation and Neutral Bond Angles and Bond Angle Differences for 1−10

		$\theta_{(CNN)}$			$\theta_{(C2-C1-C3)}$			$\theta_{(C5-C6-C4)}$[a]		
entry	substituent	C	N	D	C	N	D	C	N	D
1	p-NO_2	180.0	124.3	−55.7	124.3	121.5	−2.8	123.7	122.5	−1.2
2	CN	180.0	124.5	−55.5	123.9	121.3	−2.6	121.1	120.3	−0.8
3	Cl	180.0	124.9	−55.1	123.3	121.0	−2.3	121.4	121.4	0.0
4	F	180.0	125.0	−55.0	123.5	121.1	−2.4	123.1	122.5	−0.6
5	H	180.0	125.0	−55.0	124.0	121.3	−2.7	121.4	120.3	−1.1
6	m-CH_3	180.0	125.0	−55.0	124.3	121.4	−2.9	117.9	118.0	0.1
7	p-CH_3	180.0	125.1	−54.9	123.1	120.7	−2.4	119.1	118.4	−0.7
8	OH	180.0	125.3	−54.7	122.6	120.5	−2.1	120.8	120.3	−0.5
9	OCH_3	180.0	125.3	−54.7	122.4	120.3	−2.1	120.3	120.0	−0.3
10	NH_2	180.0	125.5	−54.5	121.7	120.0	−1.7	119.2	118.8	−0.4

[a] For the *m*-CH_3 substituted compound, the entries are $\theta_{(C6-C4-C2)}$ angles.

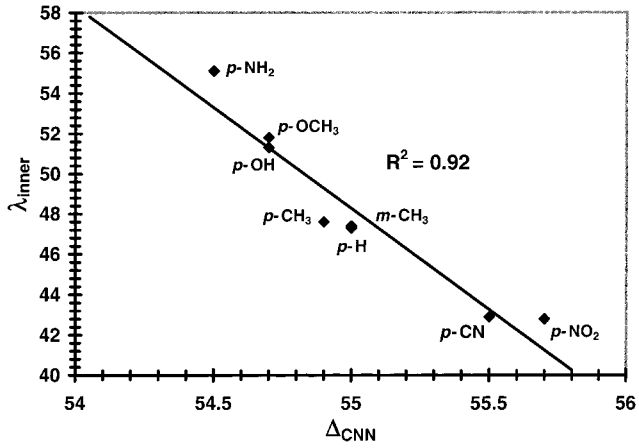

Figure 6. Plot of neutral B3LYP/6-31G* calculated θ_{CNN} relative to calculated λ_{inner}. Data are presented as the difference from 180° (θ_{CNN} for the cation).

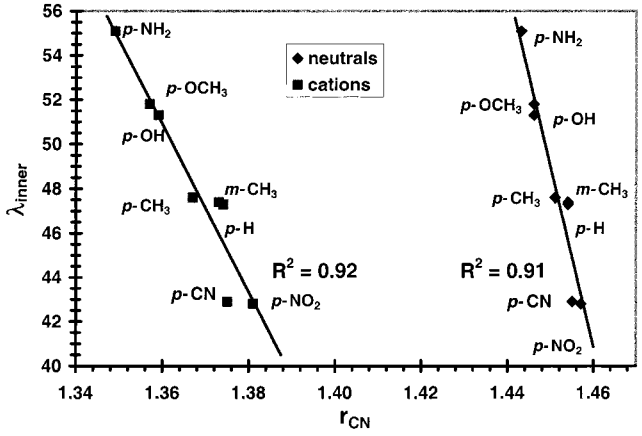

Figure 7. Plot of cation and neutral B3LYP/6-31G* calculated r_{CN} relative to calculated λ_{inner}.

about the substituent and the diazo moiety. Both of these angles are truncated in the presence of donating groups, with the C4−C6−C5 (θ_{CCC1}) angle showing the greatest range of values in the neutral (118.8−122.5°). In the cation, the C2−C1−C3 (θ_{CCC2}) angle shows the largest tendency to be affected by the substituent (121.7−124.3°), again with the smaller angles arising in donor-substituted compounds. Donating groups, such as NH_2, result in attenuated C−N bond lengths in both the neutral and cation species, with the most pronounced effect observed for the latter. Thus, as the electron-donating capacity of the substituent increases, r_{CN} shortens. This can be readily understood in resonance terms (Figure 8).

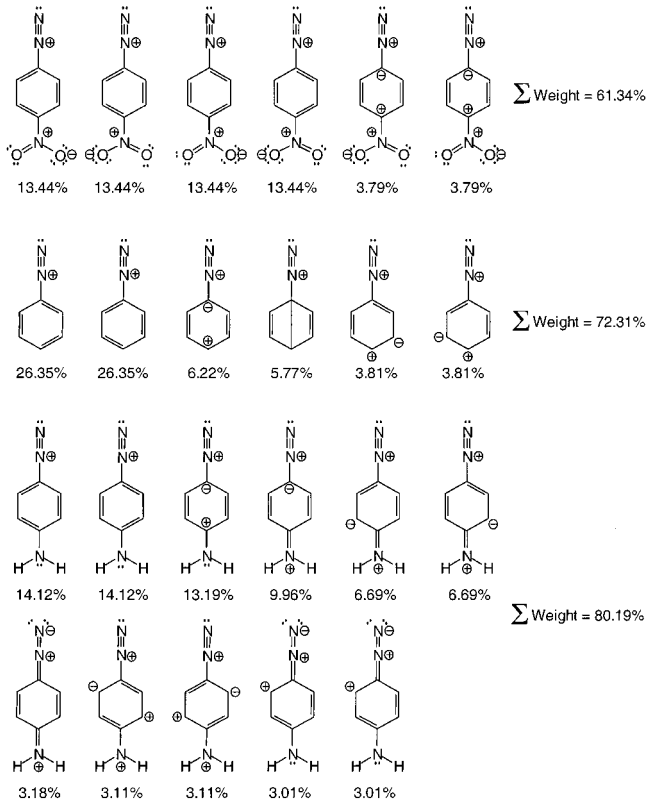

Figure 8. NRT-derived major resonance contributors for **1**, **5**, and **10**.[44]

NRT[43] analysis reveals no significant Lewis structures involving the diazo moiety that could contribute to the observed reorganization energy trends.[44] As expected, the major resonance contributors were the two Kekulé structures of the aromatic ring. A third, major resonance contributor was observed in which a negative charge was localized at C1, leaving a positive charge at C6 in each para-substituted compound. Thus, and as expected, the NRT analysis reveals that the major resonance contributors in **10** place more electron density on C1 than for **1**. This gives rise to more pronounced double bond character in r_{CN} for **10** as compared to **1**. As a substituent becomes more electron donating, the number of major resonance forms increases as well as the number of resonance forms

(43) (a) Glendening, E. D.; Weinhold, F. *J. Comput. Chem.* **1998**, *19*, 593. (b) Glendening, E. D.; Weinhold, F. *J. Comput. Chem.* **1998**, *19*, 610. (c) Glendening, E. D.; Weinhold, F. *J. Comput. Chem.* **1998**, *19*, 628.

(44) We arbitrarily define a dominant resonance structure as any that contributes 3% or more resonance weight to the composite structure.

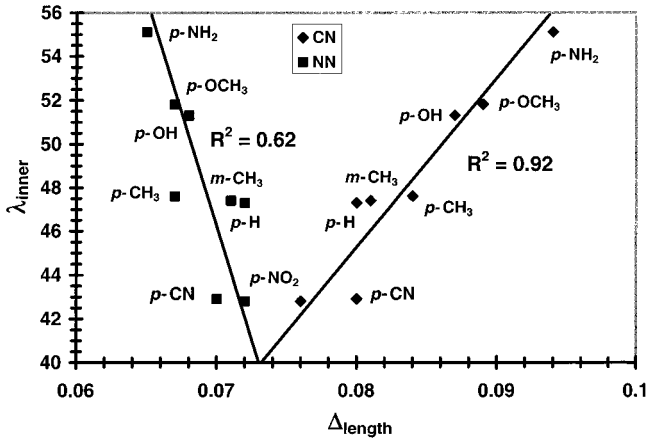

Figure 9. Plot of B3LYP/6-31G* calculated geometry changes upon SET for r_{CN} and r_{NN} relative to calculated λ_{inner}.

that increase the electron density at C1. Qualitatively, the rate of electron transfer should therefore be faster for **1** compared to **10**, simply because the diazo nitrogen in **1** is more electron deficient than in **10**. The greater double bond character of r_{CN} in **10** should also retard the rate of electron transfer because geometric reorganization to the bent diazenyl radical should be difficult to achieve.

Finally, changes in r_{CN} and θ_{CNN} upon reduction show an excellent correlation with λ_{inner}, but the correlation with r_{NN} is not as significant (Figures 6 and 9). Analysis of the changes in geometry for the series suggests that r_{CN} and θ_{CNN} are the two most important geometric parameters that change upon electron transfer. Changes in r_{NN}, r_{CX}, and θ_{CCC1} are of lesser importance, but still show moderate correlations with λ_{inner}. None of the other geometric parameters change in a predictable or correlated manner, although they almost certainly have some impact on λ_{inner}.

Conclusion

For nonhalogenated species, B3LYP/6-31G* qualitatively reproduces the experimental trends, but fails to quantitatively reproduce λ_{inner} values. Given that full valence CASSCF calculations are often necessary to quantitatively calculate λ_{inner}, this remains a reasonable compromise for qualitatively modeling geometry reorganization upon SET. Even small effects as a function of substituent were modeled effectively. In general, the DFT methods proved superior to the other methods examined, although the ROHF/6-31G* survey also showed some promise. Unfortunately, the ROHF/6-31G* data could not accurately account for small substituent effects.

For the specific cases examined, the closed-shell cation geometries showed the expected geometry about the CNN bond, with variations in the CN and NN bond lengths correlating with the electron-donating/withdrawing capacity of the substituent. As predicted by Doyle et al., a large geometry change was observed upon reduction. The neutral diazenyl radicals showed a nominal CNN bond angle of 120° and variations in the CN and NN bond lengths also correlated with the electron-donating/withdrawing capacity of the substituent. Changes in θ_{CNN} and r_{CN} both correlate well with calculated λ_{inner}. Analysis of the geometry changes for the series suggests that these two geometric parameters are the most important in determining the barrier to SET.

Acknowledgment. We gratefully acknowledge support from NIH, UIUC Research Board, Petroleum Research Fund, Critical Research Initiatives, and the IBM SUR program. Useful discussions with Lynne Miller-Deist, Jane Owens, and Jeff Vessels of the Petillo group and Professor Eric Glendening (Indiana State University) are acknowledged. P.A.P. would also like to acknowledge the encouragement and thoughtful discussions with Professor Stephen F. Nelsen (University of Wisconsin—Madison) during the course of this project.

Supporting Information Available: Gaussian 92/94 archives for calculations performed on compounds **1**—**10**. This information is available free of charge via the Internet at http://pubs.acs.org.

JO0011742